Available online at www.sciencedirect.com

SciVerse ScienceDirect

Journal of the European Ceramic Society 32 (2012) 931–935

www.elsevier.com/locate/jeurceramsoc

Optical and mechanical properties of Mg-doped sialon composite with La_2O_3 as additive

Zhangfu Yang [a], Hao Wang [a,*], Xinmin Min [a], Weimin Wang [a], Zhengyi Fu [a], Soo Wohn Lee [b], Koichi Niihara [c]

[a] State Key Lab of Advanced Technology for Materials Synthesis and Processing, Wuhan University of Technology, Wuhan 430070, China
[b] Department of Environmental Engineering, Sun Moon University, Chungnam 336-708, Republic of Korea
[c] Extreme Energy-Density Research Institute, Nagaoka University of Technology, 1603-1 Kamitomioka, Nagaoka, Niigata 940-2188, Japan

Received 27 March 2011; received in revised form 1 October 2011; accepted 16 October 2011
Available online 8 November 2011

Abstract

Using 0.5 wt.% La_2O_3 as a sintering additive, Mg-doped sialon composite with the maximum infrared transmittance of 50% was fabricated by hot pressing at 1800 °C. The addition of La_2O_3 significantly promotes the densification process of Mg-doped sialon and the anisotropic growth of β-sialon grains. As a result, the sintered material exhibits high hardness (20.2 GPa), fracture toughness (4.8 MPa $m^{1/2}$) and flexural strength (664 MPa). Furthermore, the nano-sized glassy phases concentrated at triple junctions have no obviously negative impact on infrared translucency of Mg-doped sialon.

Keywords: Sialon; Sintering; Microstructure-final; Optical properties

1. Introduction

Sialons are Si_3N_4-based solid solutions, where silicon and nitrogen are partially replaced by aluminum and oxygen.[1] They exist in two polymorphic forms, α and β, with the same hexagonal crystals but different stacking sequences along *c* axes.[1] Compared with β-sialon, α-sialon can still accommodate stabilizing cations M into its structure, where M is Li^+, Mg^{2+}, Ca^{2+}, or one of most rare earth cations, thus providing an excellent opportunity to prepare fully dense α-sialon or α/β-sialon ceramics with a reduced amount of grain-boundary phase by transient liquid sintering.[2]

In the past decades, sialon ceramics have been extensively investigated for structural engineering applications due to their excellent mechanical, thermal and chemical properties.[1] Recently, optical translucency of sialon ceramics has attracted intensive interest.[2–10] It is generally assumed that full densification and little residual grain-boundary phase should be simultaneously satisfied for achieving high transmittance in sialon.[2,6,11] Based on the point of view, considerable efforts have been made to reduce the amount of grain-boundary phase as far as possible in fully dense sialon ceramics.[2,4,6–8,10,12] To date, various single-phase α-sialon ceramics doped with single or dual cations, including Li^+, Gd^{3+}, Dy^{3+}, Y^{3+}, Lu^{3+}, Y^{3+}/Yb^{3+}, Ca^{2+}/Nd^{3+}, etc.,[2,6–8,10,12] have been fabricated with high transmission, especially in the ranges of near and middle infrared wavelength. In addition, translucent α-sialon ceramics reinforced by elongated β-sialon and/or AlN polytypoid grains such as Y-α/β-sialon were developed.[5] As mentioned above, Mg^{2+} can also be incorporated into the α-sialon lattice. In most cases, however, the densification of Mg-stabilized sialon is extremely difficult by conventional sintering methods like hot pressing due to the absence of high-temperature liquid.[13,14] The fully dense Mg-stabilized sialon with high transmittance was only obtained by spark plasma sintering at 1850 °C so far.[15]

On the other hand, owing to low viscosity of La-containing liquid, La_2O_3 has been widely used as a sintering additive to densify α-sialon ceramics.[13,16,17] Moreover, La_2O_3 can also promote the development of elongated grains, resulting in the improvement of fracture toughness.[17,18] However, the research by Kuang et al. indicated that La^{3+} could not be absorbed into the interstitial sites of α-sialon when combined with Mg^{2+} although

* Corresponding author. Tel.: +86 027 87160401; fax: +86 027 87160401.
E-mail address: shswangh@whut.edu.cn (H. Wang).

0955-2219/$ – see front matter.
doi:10.1016/j.jeurceramsoc.2011.10.020

a very small amount of La^{3+} have been observed in Ca^{2+}- or Yb^{3+}-doped α-sialon grains.[2,13] This means that addition of La_2O_3 would readily yield residual grain-boundary phase in Mg-doped sialon after sintering, and thereby deteriorate its optical properties. However, some literatures have indicated that the light scattering in composite could be negligible when the size of grain or other phase is far smaller than the wavelength of incident light.[19,20] For example, Beall et al. suggested that transparent two-phase glass-ceramic could be prepared when the size of the crystallites was smaller than 0.1 μm.[19] Jiang et al. reported that Y_2O_3–MgO nanocomposite possessed high infrared transmittance above 80% in the wavelength range of 3–7 μm although there was a large difference in the refractive indices between Y_2O_3 and MgO.[20] Hence, we believe that it is possible to achieve high translucency in Mg-doped sialon with La_2O_3 as a densification aid if residual intergranular phase is mainly concentrated on nanometer scale at triple pockets. In this work, the authors report that translucent Mg-stabilized α/β-sialon composite was fabricated by hot pressing with 0.5 wt.% La_2O_3 as a sintering additive. The influence of La_2O_3 on phase composition, microstructure, optical, and mechanical properties is investigated as well. The present study is expected to give a new approach to obtain the sialon ceramics with a good combination of optical and mechanical properties by adding an appropriate amount of sintering aids.

2. Experimental procedure

The composition investigated here was located on the α-sialon plane and represented by the formula $Mg_{m/2}Si_{12-(m+n)}Al_{m+n}O_nN_{16-n}$ with $m = 0.8$, and $n = 1.0$. Starting powders of α-Si_3N_4 (E-10, Ube Industries, Japan), AlN (F grade, Tokuyama Co., Japan), Al_2O_3 (AKP-50, Sumitomo Chemical, Japan) and MgO (Shanghai chemical, Shanghai, China) were used. The residual oxygen in α-Si_3N_4 and AlN was taken into account. 0.5 wt.% La_2O_3 (Shanghai chemical, Shanghai, China) of the weight of mixture was added to reach complete densification. The powder mixture was ball milled in absolute alcohol for 24 h with Si_3N_4 milling media, and then dried at 70 °C in a rotary evaporator.

20 g of the mixed powders was hot pressed in a graphite resistance furnace at 1800 °C for 1 h under a 0.1 MPa nitrogen atmosphere, with a uniaxial pressure of 30 MPa. A heating rate of 8 °C/min was applied between 1400 °C and 1800 °C. After sintering, the sample was naturally cooled inside the furnace. For comparison, the sample without La_2O_3 was also investigated under identical conditions. The samples without and with La_2O_3 were named as M08 and M08L, respectively.

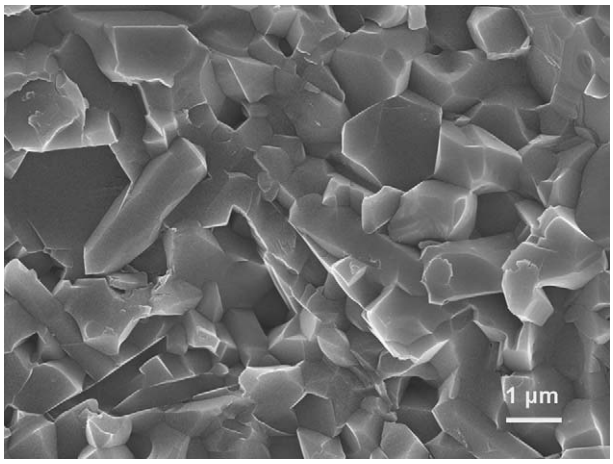

Fig. 1. SEM micrograph of fracture surface of the sample with 0.5 wt.% La_2O_3.

The as-sintered samples were ground and then polished on both surfaces. Densities of the samples were measured according to Archimedes principle. Phase assemblage was identified by X-ray diffractometry (XRD; Model D/MAX-RBX, Rigaku Co., Tokyo, Japan) with CuKα radiation. Lattice parameters were determined by XRD using Si as an internal standard. The actual solubility x of Mg^{2+} in α-sialon $Mg_xSi_{12-(m+n)}Al_{m+n}O_nN_{16-n}$ was calculated following the formula reported by Cai et al.[21] Microstructure was characterized by scanning electron microscopy (SEM; S-3400, Hitachi, Japan). Selected area electron diffraction (SAED) was conducted under transmission electronic microscopy (TEM; Model 2010F, JEOL, Tokyo, Japan). High resolution transmission electron microscopy (HRTEM) and high-angle annular dark-field scanning transmission electron microscopy (HAADF-STEM, Model TECNAI G2 F20, FEI Co., Eindhoven, Netherlands) attached with energy dispersive X-ray spectroscopy (EDS) were used to observe grain boundaries. Infrared transmittance was investigated using Fourier transform infrared spectrometer (FTIR; ThermoNicolet Nexus, Waltham, MA). Flexural strength was measured on bars (3 mm × 4 mm × 36 mm) using a three-point bend fixture with a span of 30 mm at room temperature. Vickers hardness and indentation fracture toughness were determined at room temperature under a load of 10 kg for 15 s.

3. Results and discussion

Bulk densities, phase assemblages and lattice parameters of the sintered samples are listed in Table 1. After sintered, the

Table 1
Density, phase assemblage, α-sialon lattice parameter and mechanical properties of Mg-doped sialon.

Sample	Density (g/cm^3)	Phase assemblage	Lattice parameter of α-sialon			H_V (GPa)	K_{IC} (MPa m$^{1/2}$)	Flexural strength (MPa)
			a (Å)	c (Å)	x_{actual}			
M08	2.96	α′/vs, 12H′/w, β′/vw	–	–	–	–	–	–
M08L	3.21	α′/vs, 12H′/w, β′/w	7.7920 (8)	5.6576 (1)	∼0.34	20.2 ± 0.2	4.8 ± 0.2	664 ± 16

α′, α-sialon; β′, β-sialon; vs, very strong; w, weak; vw, very weak; H_V, hardness; K_{IC}, fracture toughness.

M08L sample reached full densification (3.21 g/cm^3), while the density of the sample without La_2O_3 was only 2.96 g/cm^3. This shows that the addition of La_2O_3 could efficiently promote the densification process of Mg-doped sialon. The XRD results indicate that α-sialon was formed as the main crystalline phase coexisting with minor amounts of AlN polytypoid and β-sialon in both samples. It should be noted, moreover, that the amount of β-sialon was increased as La_2O_3 was added. The calculated x value of α-sialon in M08L is 0.34, which is less than the nominal one of 0.4. This implies that some Mg^{2+} cation may be dissolved into AlN polytypoid and/or left at the intergranular phase since β-sialon is not able to accommodate any stabilizing cations.

SEM micrograph of fractured surface of the M08L sample is indicated in Fig. 1. As shown, a small proportion of elongated β-sialon and AlN polytypoid grains are dispersed in the dense matrix of approximately equiaxed α-sialon grains. Occasionally, fine elongated β-sialon grains with high aspect ratio can also be observed. TEM image of the M08L sample is illustrated in Fig. 2(a), where the fine elongated grains with approximately 0.2 μm in width and 1 μm in length are identified as 12H by SAED. The corresponding EDS spectrum (Fig. 2(b)) further indicates that the AlN polytypoid consists of Mg besides Al, Si, O and N and then is denoted as 12H′ in terms of the literature.[13] In addition, the EDS pattern of α-sialon is given in Fig. 2(c), in which there is no signal for La, suggesting that La was hardly incorporated into the matrix. Fig. 3(a) shows STEM image of the M08L sample. It can be seen that the bright La-rich phases with a size of <50 nm primarily concentrate at some triple grain junctions since larger average atomic number results in brighter contrast. The EDS result (see Fig. 3(b)) demonstrates that the La-rich phase consists of La, Mg, Si, Al, O and N. According to the literature,[13,17] the La-rich phase is believed to be glassy rather than crystalline. However, there is no or little glassy phase at the most interfaces between grains, as further described by HRTEM image (Fig. 3(c)). Similar microstructure was also observed in Sc/Lu-doped α-sialon with an excess of 2 wt.% Sc_2O_3/Lu_2O_3.[11]

In general, penetration of liquid to grain boundaries is determined by the ratio of the solid–solid interfacial energy γ_{ss} to solid–liquid interfacial energy γ_{sl} and the corresponding dihedral angle Ψ.[22] Isolated liquid phases are formed and partially penetrate the triple-grain conjunctions when the Ψ value is more than 60°. Kleebe reported that there were clean interfaces at room temperature versus wetted grain boundaries at elevated temperature in the β-sialon (Si_5AlON_7) ceramic.[23] It has been demonstrated that the dewetting phenomenon was caused by the increase in solid–liquid interface energy when a slow cooling rate was applied. In the present work, the addition of La_2O_3 enhances the densification of Mg-doped sialon and anisotropic growth of β-sialon. It is believed, therefore, that there may be the similar wetting–dewetting behavior between grains when the Mg0810L sample was cooled on normal condition.

The infrared transmittance curve of M08L sample with 0.5 mm in thickness in the wavelength range of 1–5 μm is shown in Fig. 4(a). The transmittance increases rapidly from ~20% at the lowest wavelength of 1 μm to ~40% at 2 μm. In the range of 2.3–4.5 μm, the sample keeps high transmittance above 45% and the maximum value reaches 50% at ~3.7 μm. Beyond the wavelength of 4.5 μm, the transmittance drastically decreases and the cutoff is ~5 μm. The optical photograph of a polished slice with a square of 12 mm × 12 mm is shown in Fig. 4(b), where the underlying text is moderately visible.

In addition to good infrared optical properties, the obtained composite also possesses high hardness (20.2 GPa), fracture toughness (4.8 MPa m$^{1/2}$) and room-temperature flexural strength (664 MPa), as listed in Table 1. The improved strength and toughness are undoubtedly attributed to high density and the

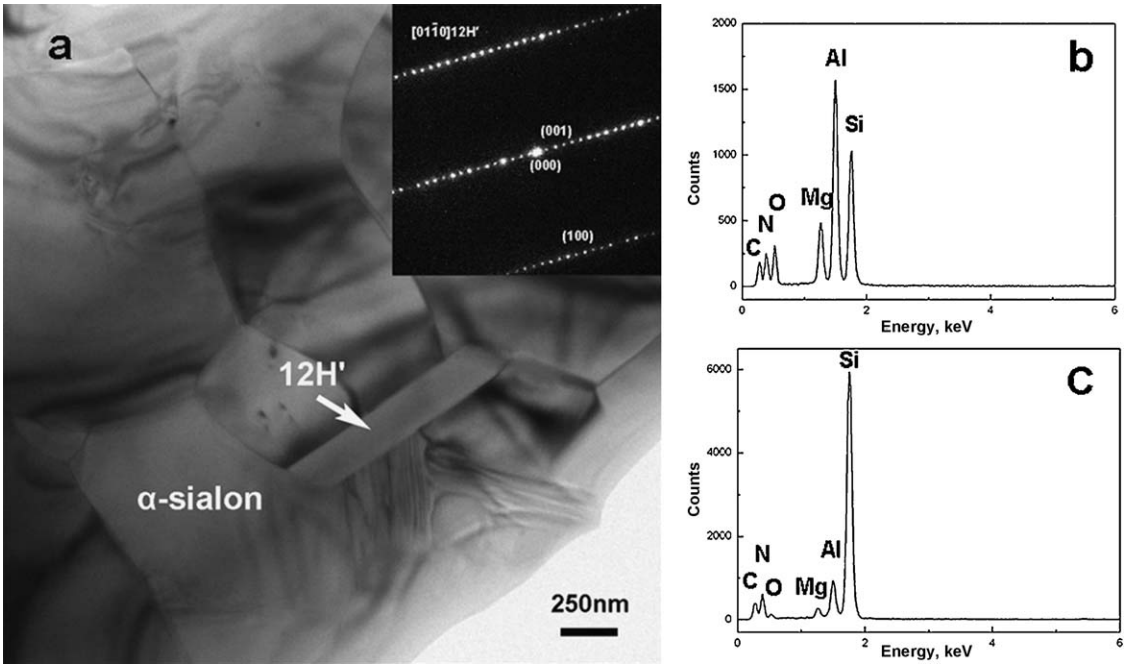

Fig. 2. (a) TEM micrograph of the sample with 0.5 wt.% La_2O_3 and the inset being SAED pattern of 12H′; EDS patterns of (b) 12H′ and (c) α-sialon.

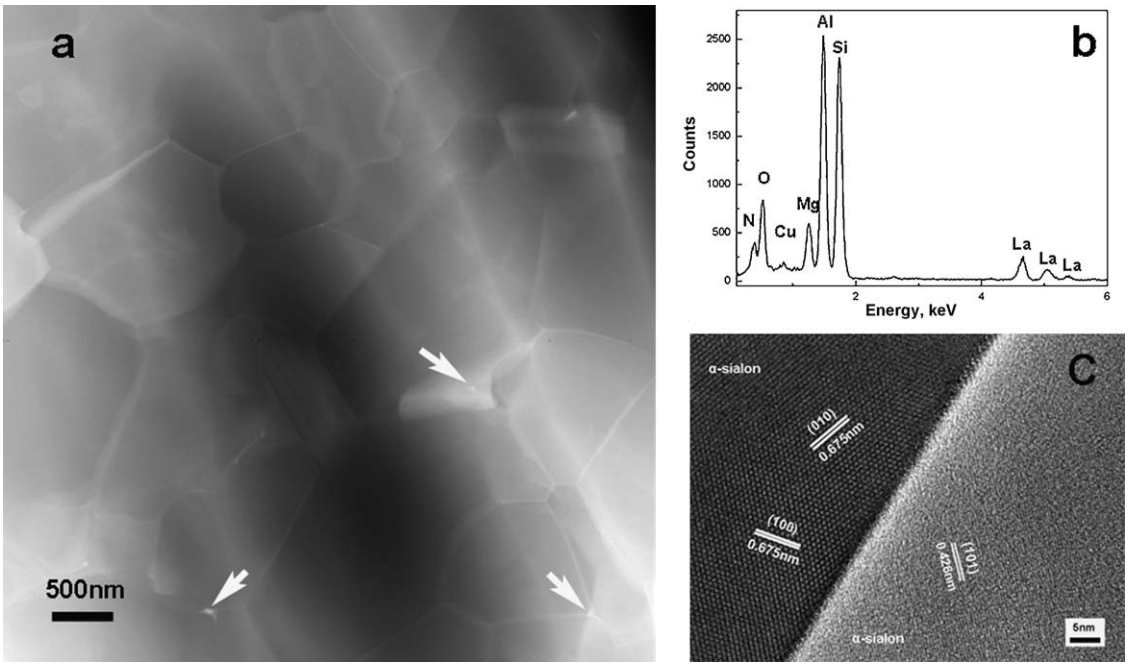

Fig. 3. (a) STEM micrograph, (b) EDS pattern of La-rich phase at triple pockets and (c) lattice fringe image of the sample with 0.5 wt.% La_2O_3.

formation of fine elongated β-sialon grains. Additionally, the composite is expected to show good high-temperature strength and oxidation resistance due to neat grain-boundary interface. The high-temperature properties are currently under investigation.

Among all α-sialons, the densification of Mg system is considered to be the most difficult because the highly refractory Mg-containing phase deprives the compact of the sintering liquid.[13,14] In this work, the Mg-doped sialon achieved satisfied densification after adding only 0.5 wt.% La_2O_3. Compared with other rare earth-containing liquid, La-containing oxynitride liquid has the lowest viscosity and the highest solubility of N due to the lowest field strength of La^{3+}.[17] Consequently, it is proposed that the densification and phase transformation of Mg-doped sialon are significantly promoted via the solution-reprecipitation mechanism in the presence of a larger amount of low-viscosity La-containing liquid phase during sintering. The increased amount of liquid could partly result from the dissolution of more metal cations like Mg^{2+} and nitrogen ions into La-containing liquid (see Fig. 3(b)). Since the addition of La_2O_3 results in the dissolution of some Mg^{2+} cations into the La-containing grain-boundary phase, the reduced amount of stabilizer in the crystalline phases gives rise to the formation of more β-sialon. As a result of a larger amount of low-viscosity La-containing liquid, the anisotropic growth of β-sialon is greatly promoted. When the sample was naturally cooled inside the furnace, the liquid phase at the two-grain junctions would migrate toward the triple-grain junctions due to the increase of solid–liquid interface energy, as mentioned above.

The loss of transmission in polycrystalline ceramics commonly comes from the light scattering centers such as residual pores, secondary crystalline phases and grain-boundary glassy phase.[2,24] In this study, the influence of pores on the optical properties could be neglected because the La_2O_3-added sample

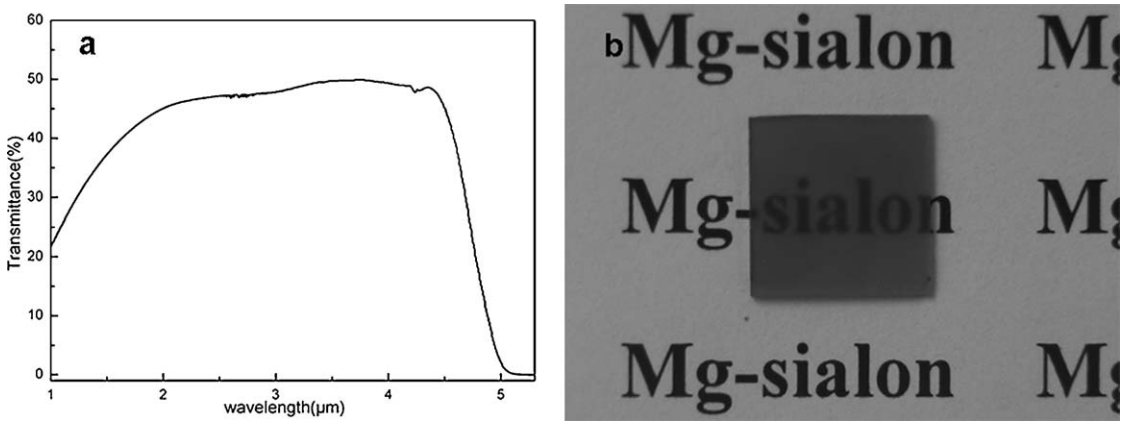

Fig. 4. (a) Optical transmittance curve and (b) appearance of the La-containing slice of 0.5 mm thickness.

achieved full densification. Due to the refractive indices similar to α-sialon, β-sialons and other secondary crystalline phases like AlN polytypoid are found not to apparently comprise the optical transmittance of translucent Y-α/β-sialon and ScLu-α-sialon, especially in the infrared region.[5,11] So the scattering caused by β-sialon and 12H′ AlN polytypoid should be low in the investigated composite. It is generally thought that grain-boundary glassy phase in sialon ceramics could seriously deteriorate the optical properties.[2] However, in the sintered Mg-doped sialon, the addition of 0.5 wt.% La_2O_3 only results in a relatively small amount of residual glassy phase. More importantly, the residual intergranular glassy phase mainly exists on nanometer scale at triple junctions. Hence, in the present work, small amounts of nano-sized glass has little effect on the middle infrared transmittance according to the proposition that the light scattering decreases with decreasing the size of scattering centers.[24] But the glassy phase as well as secondary crystalline phases still probably gives rise to scattering in the near infrared region to some extent, i.e., the wavelengths of less than 2 μm, as illustrated in Fig. 4(a). Similar observations were reported in the literature on transparent glass-ceramic and Y_2O_3–MgO.[19,20]

4. Conclusions

In summary, the addition of 0.5 wt.% La_2O_3 significantly promotes the densification process of Mg-doped sialon and the growth of elongated β-sialon grains, which result in excellent mechanical properties. In addition, the sample achieves relatively high infrared transmittance. The results indicate that a small amount of nano-sized grain-boundary glassy phase has no obviously negative impact on the middle infrared translucency of Mg-doped sialon. The capability to prepare sialon ceramics composite with a combination of good optical and mechanical properties would further widen their applications.

Acknowledgements

This research was financially supported by National Natural Science Foundation of China (A3 Foresight Program-50821140308), National High-Tech R&D Program of China (863 Program-No. 2007AA03Z527) and Specialized Research Fund for the Doctoral Program of Higher Education of China (SRFDP-No. 20090143110010).

References

1. Cao GZ, Metselaar R. α′-Sialon ceramics: a review. *Chem Mater* 1991;**3**:242–52.
2. Mandal H. New developments in α-sialon ceramics. *J Eur Ceram Soc* 1999;**19**:2349–57.
3. Karunaratne BSB, Lumby RJ, Lewis MH. Rare-earth-doped α′-sialon ceramics with novel optical properties. *J Mater Res* 1996;**11**: 2790–4.
4. Rosenflanz A. Glass-reduced SiAlONs with improved creep and oxidation resistance. *J Am Ceram Soc* 2002;**85**:2379–81.
5. Jones MI, Hyuga H, Hirao K. Optical and mechanical properties of α/β composite sialons. *J Am Ceram Soc* 2003;**86**(3):520–2.
6. Jones MI, Hyuga H, Hirao K, Yamauchi Y. Highly transparent Lu-α-sialon. *J Am Ceram Soc* 2004;**87**(4):714–6.
7. Su XL, Wang PL, Chen WW, Zhu B, Cheng YB, Yan DS. Translucent α-sialon ceramics by hot pressing. *J Am Ceram Soc* 2004;**87**(4): 730–2.
8. Chen WW, Su XL, Wang PL, Yan DS, Cheng YB, Watari K. Optical properties of Gd-α-sialon ceramics: effect of carbon contamination. *J Am Ceram Soc* 2005;**88**(8):2304–6.
9. Xue JM, Liu Q, Gui LH. Lower-temperature hot-pressed Dy-alpha-sialon ceramics with an LiF additive. *J Am Ceram Soc* 2007;**90**(5): 1623–5.
10. Ye F, Liu LM, Liu CF, Zhang HJ, Zhou Y, Yu J. High infrared transmission of Y^{3+}–Yb^{3+}-doped α-sialon. *Mater Lett* 2008;**62**(30):4535–8.
11. Ye F, Liu C, Liu L, Zhou Y. Optical properties of in situ toughened ScLu-α-SiAlON. *Scripta Mater* 2009;**61**:982–4.
12. Yang ZF, Wang H, Min XM, Wang WM, Fu ZY, Lee SW, et al. Translucent Li-α-sialon ceramics prepared by spark plasma sintering. *J Am Ceram Soc* 2010;**93**(11):3549–51.
13. Kuang SF, Huang ZK, Sun WY, Yen TS. Phase relationships in the system MgO–Si_3N_4–AlN. *J Mater Sci Lett* 1990;**9**:69–71.
14. Menon M, Chen IW. Reaction densification of alpha-sialon. II: densification behavior. *J Am Ceram Soc* 1995;**78**(3):553–9.
15. Xiong Y, Fu ZY, Wang H, Wang WM, Zhang JY, Zhang QJ, et al. Translucent Mg-alpha-sialon ceramics prepared by spark plasma sintering. *J Am Ceram Soc* 2007;**90**(5):1647–9.
16. Huang ZK, Liu SY, Rosenflanz A, Chen I-W. Sialon composites containing rare-earth melilite and neighboring phases. *J Am Ceram Soc* 1996;**79**(8):2081–90.
17. Shuba R, Chen I-W. Refractory alpha-SiAlON containing La_2O_3. *J Am Ceram Soc* 2006;**89**(9):2860–8.
18. Kim J, Rosenflanz A, Chen I-W. Microstructure control of in-situ-toughened alpha-SiAlON ceramics. *J Am Ceram Soc* 2000;**83**(7): 1819–21.
19. Beall GH, Duke DA. Transparent glass-ceramics. *J Mater Sci* 1969;**4**:340–52.
20. Jiang DT, Mukherjee AK. Spark plasma sintering of an infrared-transparent Y_2O_3–MgO nanocomposite. *J Am Ceram Soc* 2010;**93**(3):769–73.
21. Cai YB, Shen ZJ, Grins J, Esmaeilzadeh S, Hoche T. Self-reinforced nitrogen-rich calcium-alpha-SiAlON ceramics. *J Am Ceram Soc* 2007;**90**(2):608–13.
22. German RM, Suri P, Park SJ. Review: liquid phase sintering. *J Mater Sci* 2009;**44**:1–39.
23. Kleebe HJ, Pezzotti G. Grain boundary wetting dewetting in $z = 1$ SiAlON ceramic. *J Am Ceram Soc* 2002;**85**(12):3049–53.
24. Apetz R, van Bruggen MPB. Transparent alumina: a light-scattering model. *J Am Ceram Soc* 2003;**86**(3):480–6.